

## Letrozole and Curcumin Loaded-PLGA Nanoparticles: A Therapeutic Strategy for Endometriosis

Saikat Kumar Jana<sup>1</sup>, Baidyanath Chakravarty<sup>2</sup> and Koel Chaudhury<sup>1\*</sup>

<sup>1</sup>School of Medical Science and Technology, Indian Institute of Technology, Kharagpur, West Bengal, India

<sup>2</sup>Institute of Reproductive Medicine, Kolkata, West Bengal, India

### Abstract

Clinical treatment of endometriosis, a common gynaecological disorder, still remains a challenge. Hormonal suppression, pain relief medication and surgical intervention are the conventional treatment modalities; however, frequent recurrence of the disease renders the results unsatisfactory. Given the fact that oxidative stress, angiogenesis, excessive matrix degradation, and aromatase activity are associated with endometriosis, we were motivated to use the combinatorial effect of two drugs, Curcumin (Cur) and Letrozole (Let) encapsulated in PLGA and test their efficacy in mice induced with the disease. The nanoparticles (NPs) were synthesized using solvent evaporation method and characterization indicated the spherical particles to be monodispersed, polymorphic, small in size with high encapsulation efficiency, without having a tendency for significant aggregation or adhesion. Following standardization, 40mg/kg body weight of NPs was administered in endometriotic mice. Oxidative stress parameters, angiogenic markers, matrix degrading molecules, estrogen levels and endometriotic lesions, were assessed and compared before and after administration. Let-Cur NPs treatment in vivo, in addition to decreasing these parameters significantly, was also successful in reducing endometrial glands and micro-vessels density in the peritoneum to a considerable extent, thereby indicating significant regression of the disease. This is a proof of concept study. Pre-clinical non-human primate studies for testing the safety and efficacy of these NPs at larger doses in endometriosis is suggested.

**Keywords:** Dual loaded nanoparticles; Endometriosis; Letrozole; Curcumin; PLGA

### Introduction

Endometriosis is a common gynaecological disorder affecting almost 10% of the women in their reproductive age [1]. It is characterized by the benign growth of endometrial tissue outside the uterus. Severe pelvic pain and infertility are the primary symptoms of the disease. The treatment of endometriosis remains a challenge since there is no cure for the disease and recurrence rate is quite high [2]. The conventional treatment options include hormonal drugs, medication for pain relief and surgical removal of endometriotic lesions. Newer therapeutic approaches are, therefore, necessary for effective management of endometriosis.

Nanoparticulate drug delivery system is being increasingly explored as an alternative option for the development of new class of drugs for endometriosis. In a recent study, immune modulatory drug immobilized onto mesoporous silica NPs have been tested in vitro on peritoneal macrophages of women with endometriosis [3]. In another study, polymeric micelles with glycolipid-like structure have been synthesized and investigated for targeted endometriosis gene therapy [4].

It is well established that oxidative stress (OS) and inflammation are associated with endometriosis [5,6]. Antioxidant therapies for effective management of reactive oxygen species (ROS) and inflammation mediated pathological abnormalities have generated considerable research interest in recent years [6]. The polyphenol curcumin (Cur) has been extensively studied for its anti-inflammatory, antioxidant, anti-carcinogenic, and anti-bacterial activities [7] and its potential as a therapeutic agent well accepted. However, its widespread clinical application has been limited due to poor aqueous solubility [8], and consequently, minimal systemic bioavailability [9]. Various groups have attempted to circumvent the pitfalls of poor solubility by developing Cur nanoparticles (NPs) [8,10,11].

Endometriosis tissues, like breast cancer, express a high level of aromatase and estrogen (E2) receptors. The enzyme aromatase converts

estrogen-precursor molecules to E2. Since endometriosis is an E2-dependent disease, it can be effectively treated by the withdrawal of E2. Aromatase inhibitors have emerged as a new therapeutic strategy against endometriosis-associated pathogenesis. Several studies have shown that letrozole (Let), an aromatase inhibitor, can reduce endometriosis-related lesions and associated pain in most of the subjects [12-14]. Combination of Let with other drugs has been tested against endometriosis [13,15].

Delivery of multiple therapeutic agents with a single drug nano carrier has generated considerable research interest in recent years. Co-delivery of multiple drugs targeting a common pathological abnormality can function synergistically with higher therapeutic efficacy and better target selectivity [16]. This motivated us to encapsulate Let and Cur in PLGA and explore the sustained release effect of these dual-loaded NPs in mice induced with endometriosis.

### Material and Methods

#### Synthesis of NPs

PLGA NPs loaded with the two drugs, Cur and Let was prepared using a modified version of an o/w single-emulsion solvent evaporation

**\*Corresponding author:** Koel Chaudhury, School of Medical Science and Technology, Indian Institute of Technology, India, Tel: 91-3222-283572, +91-9434341334; Fax: 91-3222-2221; E-mail: [koel@smst.iitkgp.ernet.in](mailto:koel@smst.iitkgp.ernet.in) or [koeliitkgp@gmail.com](mailto:koeliitkgp@gmail.com)

**Received** January 12, 2013; **Accepted** January 27, 2014; **Published** January 29, 2014

**Citation:** Jana SK, Chakravarty B, Chaudhury K (2014) Letrozole and Curcumin Loaded-PLGA Nanoparticles: A Therapeutic Strategy for Endometriosis. J Nanomedicine Biotherapeutic Discov 4: 123. doi:10.4172/2155-983X.1000123

**Copyright:** © 2014 Jana SK, et al. This is an open-access article distributed under the terms of the Creative Commons Attribution License, which permits unrestricted use, distribution, and reproduction in any medium, provided the original author and source are credited.

process [17]. The organic phase consisted of PLGA polymer and the aqueous phase contained the polyvinyl alcohol (PVA) solution. The drugs were dissolved in an acetone - dichloromethane mixture. The organic phase was emulsified with the aqueous phase by sonication using a micro tip probe sonicator (Hielscher Ultrasonics GmbH, Germany) at an output of 50W for 30s in an ice bath. The organic mixture was then rapidly removed by evaporation at 37°C leaving behind colloidal suspension of PLGA NPs (Cur-Let-PLGA-NPs) in water. All experiments were conducted by varying one of the parameters, keeping the remaining process parameters at standard conditions: 200 mg/ml of PLGA 75:25, MW 15 kDa, 10 mg Cur and 10 mg Let in 1.5 ml of acetone-dichloromethane mixture (1:2, v/v) as the organic phase, and 4.5 ml of 2% PVA solution as the aqueous phase. All batches of NPs were produced in triplicate. The same conditions were followed for the preparation of Let-NPs and Cur-NPs.

### Particle size and zeta potential

Dynamic light scattering (DLS) measurements for determining the average size and size distribution of the NPs were performed using a Nanosizer 90 ZS (Malvern Instruments Ltd., Malvern, UK) at 25°C. The intensity of scattered light was detected at 90° to the incident beam. The freeze-dried Let-Cur-NP powder was dispersed in water and measurements carried out following which the solution was filtered with a micro filter having an average pore size of 0.2 µm (Millipore). Zeta potential was measured at 25°C using the same instrument. The average size and charge distribution of Let-NPs and Cur-NPs were also recorded. Data analysis was done in the automatic mode. The measured size is presented as the average value of 20 runs, with triplicate measurements within each run.

### Scanning electron microscopy

A concentrated aqueous suspension of Let-Cur-NPs was spread over a slab and dried under vacuum and coated with gold. The morphology of NPs in each field was calculated using scanning electron microscopy (SEM; JEOL JSM-6700F, Tokyo, Japan) operating at 5keV. The experiment was repeated for Let-NPs and Cur-NPs.

### Fourier transforms infrared spectroscopy

Fourier transform infrared (FTIR) spectroscopy was used to determine the interaction and bonding between PLGA and the encapsulated drugs using a Perkin- Elmer 2000 spectrophotometer (Perkin-Elmer, Norwalk, CT). Potassium bromide (KBr) was mixed with Let- Cur-NP powder and ground by an agate mortar to be finally compressed into a thin tablet. The experiment was repeated for Let-NPs and Cur-NPs. The study was done in triplicate with the scanning range set between 400 and 4000 cm<sup>-1</sup>.

### Encapsulation efficiency

The purified drug-loaded freeze-dried NPs recovered were suspended in 5 ml of distilled water, mixed together for 1 h, and finally subjected to centrifugation at 20,000 rpm at 25°C for 30 min. The amount of drug present in the supernatant as well as dissolved NPs were analyzed by HPLC with absorbance at 450 nm and 238 nm for curcumin and letrozole, respectively. A standard calibration curve was constructed using different concentrations of the drug versus maximum absorbance. Encapsulation efficiency was calculated using the following formula:

$$\text{Encapsulation efficiency (\%)} = \frac{\text{Encapsulated drug} - \text{Free drug}}{\text{Total drug}} \times 100$$

### In-vitro release

Lyophilized polymeric NPs were dispersed in 10 ml PBS (pH 7.4) and the solution divided in 20 microfuge tubes (500 µl each). The tubes were kept in a thermostable water bath set at room temperature (RT). The solution was centrifuged at 3000 rpm at different intervals of time to separate released (pelleted) Cur and Let which were re-dissolved in 1 ml of acetone and the absorbance measured by HPLC at 450 nm and 238nm, respectively. Concentration of the released Cur and Let was then calculated using the standard curve of the respective drugs. The percentage of Cur and Let released was determined from the following equation:

$$\text{Release (\%)} = \frac{[\text{Drug}] \text{ release}}{[\text{Drug}] \text{ total}} \times 100$$

where [Drug] release is the concentration of released Cur and Let collected at time t and [Drug] total is the total amount of Cur and Let entrapped in the NPs.

### Cytotoxicity assay

Cell proliferation/cytotoxicity was estimated by colorimetric assay using MTT dye in mice fibroblast (3T3) cell line. Cells were cultured in 96-well plate at a density of 3×10<sup>3</sup> cells/well, treated with different concentration of NPs and incubated for 24 h. MTT was added to the cells at a final concentration of 1.2mM and incubated for 4h. Cells were lysed and insoluble formazan product dissolved using buffer (10% SDS, 0.1M HCl). Absorbance of each well was measured using spectrophotometry (Victor X3, Perkin Elmer, USA). Cell proliferation was calculated by taking absorbance of NP-treated samples and untreated controls and expressed as a percentage.

### Animals

CD-1 strain Swiss Albino female mice weighing 31 ± 3 g and 5-6 weeks of age were used in this study. These mice were maintained at 14-h light and 10-h dark photoperiod under constant temperature (25° ± 2°C) and provided with standard food and water, ad libitum according to the guidelines of Committee for the Purpose of Supervision and Control of Experiments on Animals, Chennai, India. Approval was obtained from the Animal Ethics Committee of the Institute to carry out this study.

### Lethal dose determination

Forty mice were randomly divided into 8 groups with 5 mice per group. NPs dissolved in saline were administered intra peritoneally at the doses indicated in Figure 1. At the end of the 14 day post-treatment period, cumulative mortality was calculated.

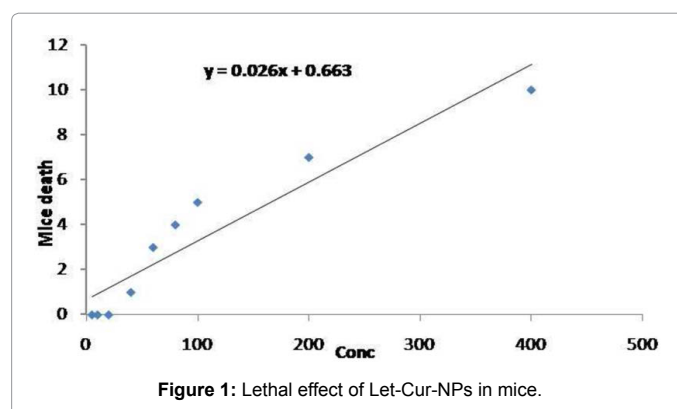
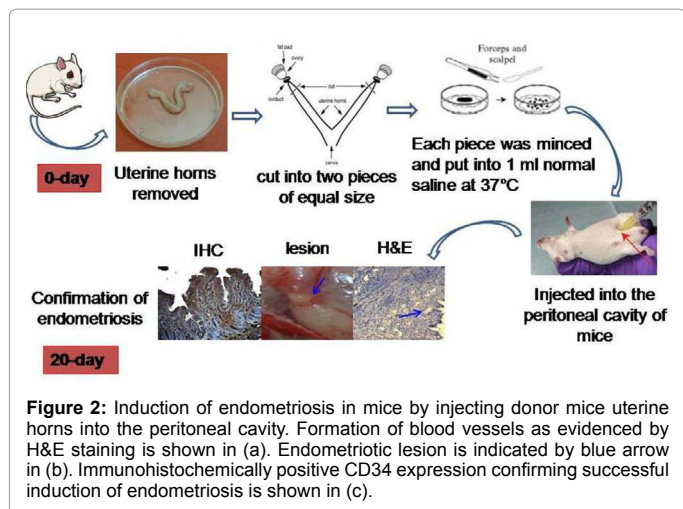


Figure 1: Lethal effect of Let-Cur-NPs in mice.



**Figure 2:** Induction of endometriosis in mice by injecting donor mice uterine horns into the peritoneal cavity. Formation of blood vessels as evidenced by H&E staining is shown in (a). Endometriotic lesion is indicated by blue arrow in (b). Immunohistochemically positive CD34 expression confirming successful induction of endometriosis is shown in (c).

### Haematological studies and biochemical parameters estimation

A fresh batch of 20 mice were taken and divided into 4 groups. 40 mg/kg of each type of NP (Cur-Let-NP, Cur-NP, Let-NP) and 0.9%NaCl was injected intraperitoneally into respective group. Blood samples were collected 15 days of post treatment. White blood cells (WBC), red blood cells (RBC), mean corpuscular volume (MCV), haemoglobin (Hb), neutrophils (NEU), lymphocytes (LYM), monocytes (MON), eosinophils (EOS), basophils (BAS) and blood platelets (PLT) were estimated using automated hematology analyzer (Sysmex KX-21N™ semi Automated Hematology Analyzer, Japan).

For biochemical parameters assessment, serum was separated from the blood samples and Alkaline phosphatase (ALP), Albumin (ALB), Globulin (GLB), Total bilirubin (TBL), Blood urea nitrogen (BUN), Creatinine (CRT), Glucose (GLU), Serum glutamate oxaloacetate transaminase (SGOT), and serum glutamate pyruvate transaminase (SGPT) estimated in an semi Auto analyzer Microlab 300 (Microlab 300, Germany) using appropriate kits.

### Animal study design

A total of 60 mice were taken for this part of the study, out of which 55 mice were induced with endometriosis and the remaining 5 healthy ones considered as controls for comparison purposes.

**Endometriosis induction and confirmation:** Endometriosis was induced according to a method reported by Nowak et al. [18], with slight modifications [18]. A schematic diagram representing the induction and confirmation of endometriosis in mice is shown in Figure 2. The endometrium fragments of two uteri of donor mice were pooled and every recipient mouse received 35 mg tissue in 300 µl DMEM. Briefly, on day 0, the donor mice were anesthetized, sacrificed by cervical dislocation and the uterine horns harvested under sterile conditions. Next, the uterine horns were cut into two pieces of equal size, each piece minced and placed in 1ml DMEM at 37°C. The uterine tissues weighing 35 mg were injected into the peritoneal cavity of the recipient animals at the midline just below the mice umbilicus, using an 18-gauge needle and the day designated as day 0. Normal saline of the same volume as that of injected uterine tissue but not containing uterine tissues was injected into the cavity of the control mice.

To confirm successful induction of endometriosis, a total of 9 mice were sacrificed at 3 observation days, i.e., 7th, 15th and 20th day, with 3

animals examined on each observation day for pelvic and intraperitoneal changes due to the induced disease. The abdominal cavity was opened, lesions randomly selected from different intraperitoneal sites, excised and processed for disease assessment and immune histo chemistry evaluation. Endometriosis was confirmed by assessing formation of new blood vessels, endometrial glands and stroma, and CD34-staining of the micro vessel structures within the endometriotic lesion. A flow chart where the study design involves induction and confirmation of endometriosis, injection of various NPs, and biochemical parameters assessment before and after NP injection is given in Figure 3.

OS markers (ROS, LPO and TAC), matrix degrading enzymes, matrix metallo proteinases (MMP-2 and MMP-9) and angiogenic marker (VEGF) were assessed in serum of endometriosis induced mice (n=5) and controls (n=5) and compared. Next, the anti-angiogenic, antioxidant, inhibitory effect on ECM degradation, and anti-estrogenic effect of Cur-Let-NPs on endometriosis were investigated. Mice induced with endometriosis were divided into 4 groups and NPs at a dose of 40 mg/kg body weight administered to the respective groups four times, at 5 days interval. Various NPs consisting of (i) Cur-Let-NPs (n=10) (ii) Cur-NPs (n=10) (iii) Let- NPs (n=10) and (iv) 0.9% NaCl (n=10) were administered into the peritoneal cavity of the abdominal wall with an 18-gauge needle on the midline just below the mice umbilicus.

Blood samples were collected from the saphenous vein of mice at D30 and D40 for estimation of OS parameters, matrix degrading enzymes, angiogenic and estrogenic parameters. After completion of study (D-40), all mice were sacrificed to visually inspect the endometriotic lesions in the peritoneal cavity and endometrial tissue

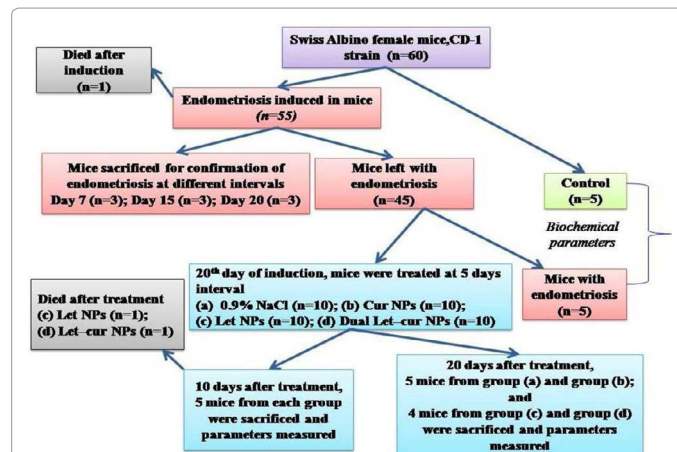


**Figure 3a:** Flow chart depicting the animal study design. The study aims to assess the effect of intraperitoneally injected cur-Let-NPs on mice with endometriosis.

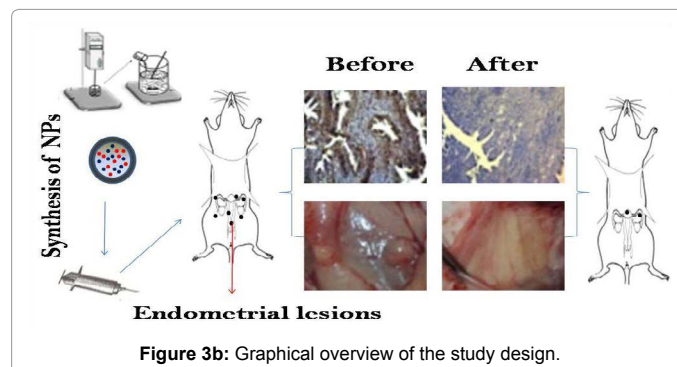


**Figure 3b:** Graphical overview of the study design.



sections collected for IHC. During the entire study period, one mouse died following induction of endometriosis and two mice with endometriosis died following NPs treatment.

### Histological examination of the peritoneal tissue

Intraperitoneal tissue sections from mice with endometriosis and controls were fixed in 4% paraformaldehyde, embedded in paraffin and sectioned. Subsequently, these tissue sections were stained with hematoxylin and eosin (H&E) and viewed under light microscopy.

### Immuno histochemistry of peritoneal tissue

Paraffin-embedded section slides were deparaffinised by xylene. Tissue sections were then rehydrated in a series of alcohol gradient (2 times in 100% for 10 min and once in 95%, 70% and 50%, each for 5 min). Next, the rehydrated tissues were washed with PBS and antigen retrieved using sodium citrate (pH 6) for 20 min at 95 °C. Non-specific regions of tissue samples were blocked using bovine serum albumin for 1 h at RT. Sections were incubated overnight at 2–8 °C with anti-mouse CD34 primary antibody (119301, Biolegend, USA). Next, tissue sections were washed thrice, each for 15 min in PBS. The sections were then incubated with secondary

antibody according to the manufacturer's protocol, before incubation with avidin biotinylated horse radish peroxidase (Santa Cruz biotechnology, INC., Santa Cruz, California, USA). Labeled cells were visualized with DAB and sections counterstained with hematoxylin. Next, the slides were dehydrated using series of alcohol gradient and mounted using DPX and xylene. The slides were then examined under bright field microscope (Carl Zeiss, Jena, Germany).

### OS parameters assessment

**Measurement of Reactive Oxygen Species:** Free radicals generation was determined in serum samples from endometriosis and controls by monitoring luminol (5-amino- 2,3-dihydro-1,4-phthalazinedione)-mediated chemiluminescence (CL)[Chaudhury et al. 2012]. Luminol reacts with ROS present in serum resulting in a luminophore that has an emission peak at ~425 nm. The intensity of the chemiluminescence is proportional to the amount of ROS in the serum. The reaction mixture contained 25 L of serum and 0.1 mM luminol in 10 mM sodium phosphate buffer (pH 7.4). The reaction was initiated by the addition of H<sub>2</sub>O<sub>2</sub> at a final concentration of 1 mM. CL was measured for 10 min using a luminometer (Berthold, Sirius Single tube Luminometer, Model No. 0727). Hydrogen peroxide was added as an activator of luminol. Background (blank) was determined in each experiment utilizing H<sub>2</sub>O<sub>2</sub>, luminol, and sodium phosphate buffer without samples. The reaction was performed at 37°C and expressed in relative light units (cps).

**Measurement of Lipid Peroxidation:** The slightly modified Thio barbituric acid (TBA) method [19] was used to measure Malonaldehyde (MDA) content in the serum sample. Fifty L aliquot of frozen serum was thawed and immediately used for lipid peroxidation (LPO) estimation. Hundred L of stock reagent (12%, w/v trichloroacetic acid, 0.375%, w/v TBA and 0.25 mol/L HCl warmed to dissolve the TBA) was mixed thoroughly with 50 L of the sample and heated for 15 min in a boiling water bath. After cooling, the flocculent precipitate was removed by centrifugation at 1000 ×g for 10 min and the OD of the supernatant determined at 535 nm using a multiplate reader (VictorX3, Perkin Elmer, USA) against a blank containing all the reagents. LPO values were expressed as M MDA.

**Measurement of Total antioxidant capacity:** Total antioxidant capacity (TAC) was measured in serum using a modified enhanced CL

assay [20]. Serum was thawed at RT and diluted 1:10 with deionized water. Signal reagent was prepared using a chemiluminescence kit (GE Healthcare, UK). A constant peak of ROS was produced using HRP conjugated IgG (Santa Cruz Biotechnology, Santa Cruz, CA). HRP was diluted with deionized water to give a desired CL output. Luminometer was set in the kinetic mode, and 900 L of reaction mixture (100 L signal reagent + 700 L deionized water + 100 L 1: 350 diluted HRP) was added to the cuvette. After 100 seconds of reaction mixture addition, 50 L of the diluted serum sample was added to the mixture, and 10% recovery of CL was recorded. Trolox, a water soluble tocopherol analogue, was used as a standard. The antioxidant capacity of serum samples was expressed in M Trolox equivalents.

**VEGF, MMPs and E2 assessment:** Serum collected from mice for OS measurements was also analyzed for VEGF, MMPs and E2 using ELISA. Serum was diluted in 50 mM carbonate buffer at pH 9.0, added to ELISA plate and left overnight at 4°C. The antigen solution was removed and 200 µL/well of blocking buffer

(PBS containing 1% BSA) added to block non-specific protein binding. After incubation for 1–2 h at RT, the wells were washed with TBS (PBS containing 0.1% Tween 20), and antibody (1:1000 dilution of 1 mg/mL stock) added followed by incubation for 2 h at RT. The wells were washed again, and 50 µL/well of goat anti-mouse alkaline phosphatase conjugated secondary antibody (sc2008, Santacruz, California) diluted to 1:1000, was added. Following incubation for one hour at RT, wells were washed three times with TBS. 50 µL/well of para nitrophenyl phosphate (Santacruz, California) dissolved in diethanolamine buffer to a final concentration of 1 mg/mL was added and allowed to develop for 10–20 min or until positive control reached an OD of about 1.0. Plate readings on microtiter plate reader were taken. Data was analyzed with respect to the standard curve of individual molecules.

## Results

### Size and charge distribution of synthesized NPs

PLGA encapsulated Cur, Let and dual-loaded NPs were successfully synthesized by solvent evaporation method. Consistency of the NPs synthesized was checked by subjecting the NPs from different batches to DLS, SEM and zeta potential measurements. The synthesized NPs were found to be completely soluble in water. The size and charge of Let-Cur-NPs, Let-NPs and Cur- NPs are shown in Figure 4 and Table 1, respectively.

### Drug-polymer interaction studies

PLGA encapsulated Let-Cur-NPs, Let-NPs and Cur-NPs were characterized using FTIR spectroscopy. FTIR spectra of Cur and Let standards were also obtained to identify the different vibrational peaks. The spectra obtained are illustrated in Figure 5 and the identified peaks summarized in Table 2. No significant differences in shape and position of the absorption peaks were observed between spectra a, b and c. Let-NPs indicates major peaks at 2232 cm<sup>-1</sup> for C≡N stretching. Further, Cur-NPs show 1027 cm<sup>-1</sup> and 1271 cm<sup>-1</sup> for -OCH<sub>3</sub> stretching and C-O stretching, respectively. PLGA associated stretching peaks including 1745 cm<sup>-1</sup> for C=O ester, 2900-3000 cm<sup>-1</sup> for C-H and 3660 cm<sup>-1</sup> for OH were present in all types of NPs synthesized.

### Surface morphology of NPs

SEM images of Let-Cur-NPs, Let-NPs and Cur-NPs are shown in Figure 6. All NPs were found to be almost spherical in shape without any significant aggregation or adhesion.

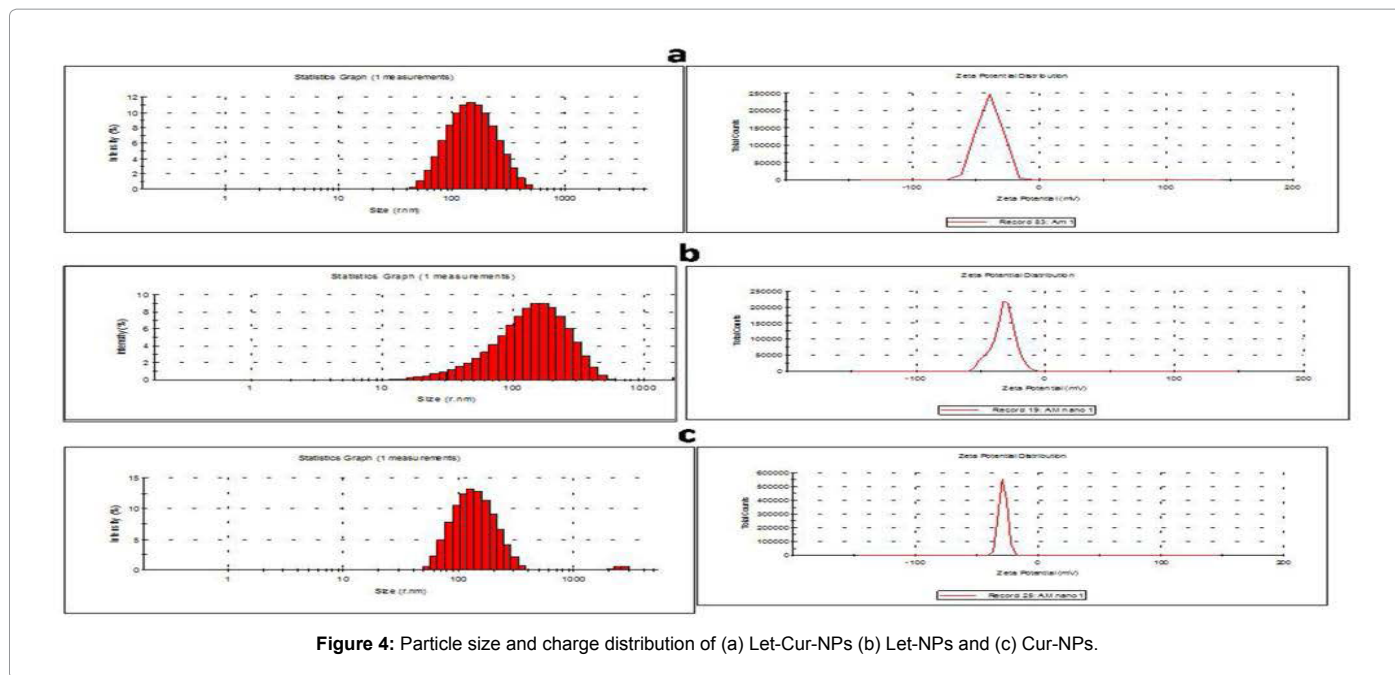


Figure 4: Particle size and charge distribution of (a) Let-Cur-NPs (b) Let-NPs and (c) Cur-NPs.

NPs	Size (nm)	Zeta Potential (mV)
Dual-NPs	127 ± 4.5	-31.60 ± 1.91
Let-NPs	115 ± 3	-27.47 ± 1.56
Cur-NPs	121.3 ± 2.5	-31.27 ± 1.45

Mean ± SEM

Table 1: Charge and size of synthesized NPs.

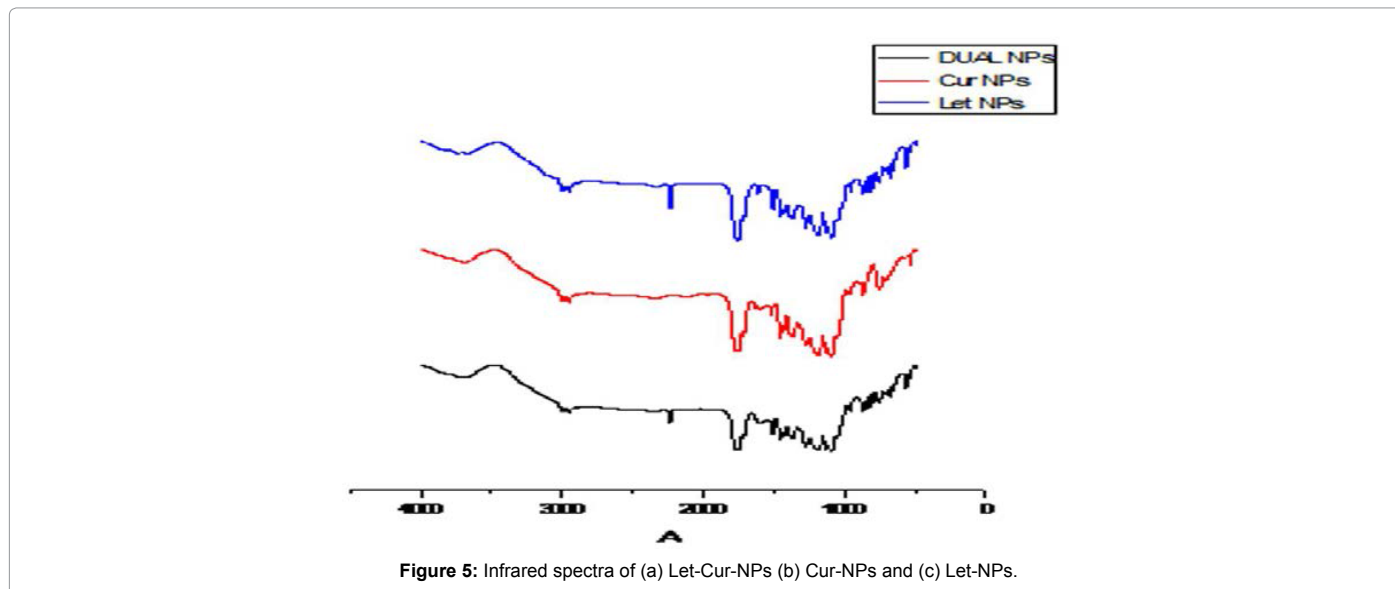


Figure 5: Infrared spectra of (a) Let-Cur-NPs (b) Cur-NPs and (c) Let-NPs.

### Encapsulation efficiency of the synthesized NPs

Entrapment efficiency of NPs was determined using HPLC. The amount of free curcumin and letrozole in the supernatant was quantified after each step of centrifugation during the synthesis of NPs. A standard calibration curve was plotted using standard concentrations of drugs dissolved in acetone. HPLC quantification was achieved by taking the absorbance at 450 nm and 238 nm. Figure 7 shows high encapsulation efficiency of the synthesized NPs.

### Cell viability assay

Cytotoxicity profile of the NPs was studied using MTT (3-(4,5 dimethylthiazol-2-yl)-2,5- diphenyl tetrazolium bromide) assay. Five different concentrations of each of the synthesized NPs were used for this study. The respective assay reagents were added after incubating the cells and the NPs for 24 h. The absorbance readings were taken and the results calculated. The results suggest that the NPs do not exert any

PLGA (cm-1)	PLGA-Cur-NPs (cm-1)	PLGA-Let-NPs (cm-1)	PLGA-Let-Cur-NPs (cm-1)
1090 C-O str.	1086 C-O str.	1340-1020 C-N (m) str.	
	1027 -OCH3 (m) str.		1036 -OCH3 (m) str.
	1271 C-O str.		1269 C-O str.
	1600 C=C str.		
	1623 C=O str.		1620 C=O str.
		2232 C≡N str.	2232 C≡N str.
1750 C=O ester	1742 C=O ester	1744 C=O ester	1745 C=O ester
2900-3000 C-H (s) str.	2900-3000 C-H (s) str.	2900-3000 C-H (s) str.	2900-3000
3650 (br) OH str.	3650 (br) OH str.	3600-3700 (br) OH str.	3660 (br) OH str.

**Table 2:** Vibrational peaks assignment of PLGA encapsulated NPs using FTIR.

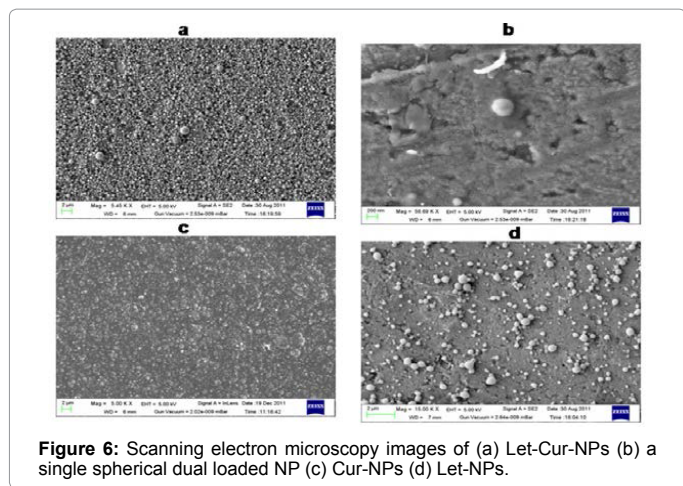


**Figure 6:** Scanning electron microscopy images of (a) Let-Cur-NPs (b) a single spherical dual loaded NP (c) Cur-NPs (d) Let-NPs.

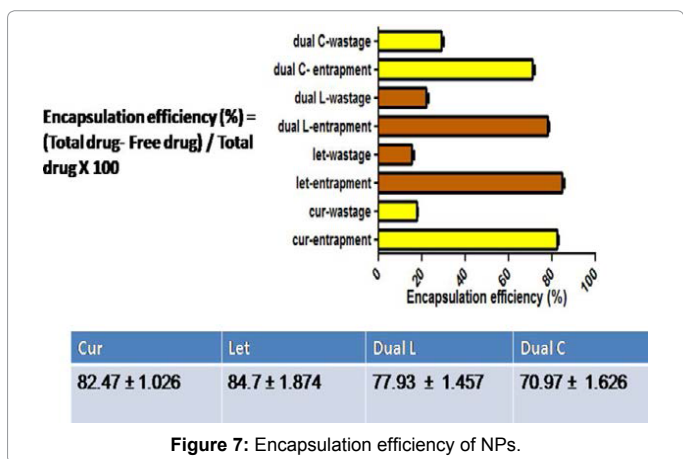


**Figure 7:** Encapsulation efficiency of NPs.

significant cytotoxic effect on normal cells (Figure 8). The cells treated with the highest concentration of NPs showed viability > 65%.

### In vitro release of drugs from NPs

In vitro release kinetics of Let-Cur-NPs, Cur-NPs and Let-NPs were studied for 8 days and shown in Figure 9. In the present formulation, drugs release occurred in a biphasic manner, with an initial burst phase followed by a slower or sustained drug release phase. Since degradation of PLGA is slow, the release of drugs from the NPs would mainly depend on the diffusion of drug through polymer. The release kinetics of Let-

Cur-NPs demonstrate ~ 25% release of Cur and ~35% release of Let from PLGA over a period of 24 h when dispersed in PBS at physiological pH. In addition, ~ 25% release of Cur from Cur-NPs and ~ 29% release of Let from Let-NPs were observed under similar conditions. The error bars represent mean and standard error of experiments performed in triplicate.

### Lethal dose

Figure 1 show the results of Let-Cur-NPs toxicity in mice. Based on the data shown in Figure 1, LD50 of dual-NPs was observed to be 850 mg /kg.

### Haematological studies

There was no observable swelling or hair loss at the abdominal implantation sites. Also, no sign of stress and anaesthesia intolerance was observed. No significant difference in weight change during the study period was observed between groups of mice. Haematological parameters in mice did not show considerable changes after administration of NPs (Table 3).

### Effect of NPs in mice with endometriosis

Figure 10 provides a representative view of the peritoneal cavity of endometriosis induced mice injected with (A) 0.9% NaCl (B) Let-Cur-NPs (C) Let-NPs and (D) Cur-NPs. Visual inspection showed no changes in the endometriotic lesions following 0.9% NaCl injection [A], whereas the lesions, blood vessels, and glands reduced considerably

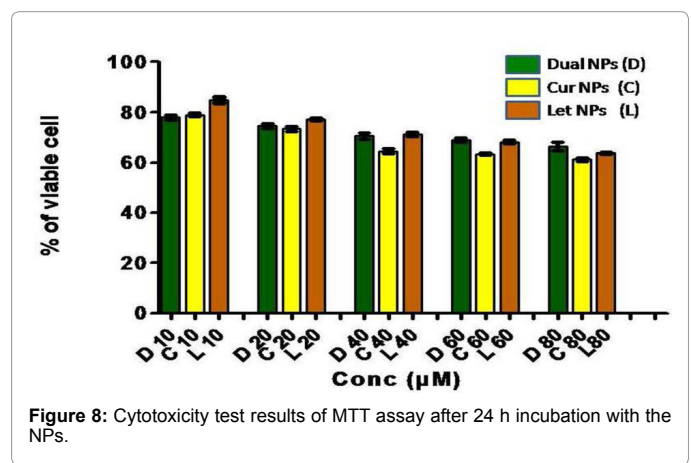


**Figure 8:** Cytotoxicity test results of MTT assay after 24 h incubation with the NPs.

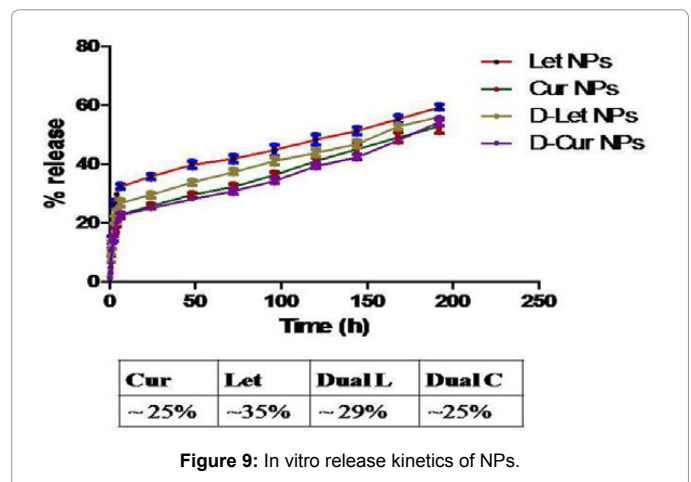


**Figure 9:** In vitro release kinetics of NPs.



Different parameters	Normal range	Control (0.9% NaCl)	Cur-NPs (40 mg/kg)	Let-NPs (40 mg/kg)	Cur-Let-NPs (40mg/kg)
RBC (x106/ $\mu$ l)	8.4-15.5	9.1 $\pm$ 1.05	11.4 $\pm$ 1.21	13.8 $\pm$ 2.15	12.9 $\pm$ 3.14
WBC (x103/ $\mu$ l)	6-15	9.2 $\pm$ 1.11	6.8 $\pm$ 1.13	10.4 $\pm$ 1.18	14.2 $\pm$ 1.15
MCV (fl)	41-49	42.7 $\pm$ 3.36	46.3 $\pm$ 3.16	47.6 $\pm$ 5.18	46.2 $\pm$ 3.53
Hb (g/dl)	10.2-16.6	12.2 $\pm$ 1.12	14.8 $\pm$ 1.12	13.8 $\pm$ 1.11	15.4 $\pm$ 1.21
NEU (x103/ $\mu$ l)	3-12	7.2 $\pm$ 0.61	7.8 $\pm$ 1.13	5.7 $\pm$ 0.14	9.1 $\pm$ 1.12
LYM	55-95%	68.6 $\pm$ 5.31	81.6 $\pm$ 1.15	75.8 $\pm$ 5.81	72.8 $\pm$ 6.81
MON	1-4%	2.1 $\pm$ 0.11	1.6 $\pm$ 0.18	2.7 $\pm$ 0.18	2.9 $\pm$ 0.12
EOS	0-4%	1.48 $\pm$ 0.12	2.1 $\pm$ 0.19	3.1 $\pm$ 0.15	2.1 $\pm$ 0.11
BAS	0-1%	0.7 $\pm$ 0.04	0.9 $\pm$ 0.01	0.64 $\pm$ 0.02	0.8 $\pm$ 0.03
PLT (x103/ $\mu$ l)	160-410	287.9 $\pm$ 21.5	339.2 $\pm$ 21.11	366.1 $\pm$ 25.41	278.8 $\pm$ 25.32
ALP (U/L)	35-96	65.2 $\pm$ 3.71	76.3 $\pm$ 2.13	81.2 $\pm$ 3.69	71.2 $\pm$ 2.51
SGOT (U/L)	50-80	74.3 $\pm$ 2.91	69.7 $\pm$ 1.33	71.3 $\pm$ 2.81	68.5 $\pm$ 2.71
SGPT (U/L)	90-120	113.1 $\pm$ 11.96	108.9 $\pm$ 11.44	98.5 $\pm$ 5.81	114.3 $\pm$ 12.98
Albumin (g/dL)	2.5-5.4	3.6 $\pm$ 0.43	4.8 $\pm$ 0.12	3.7 $\pm$ 0.13	4.1 $\pm$ 0.16
GLB(mg/dL)	46-279	172.9 $\pm$ 12.11	94.3 $\pm$ 6.81	184.7 $\pm$ 19.22	176.8 $\pm$ 12.64
TBL (mg/dL)	0.1-1.1	0.5 $\pm$ 0.21	0.6 $\pm$ 0.12	0.9 $\pm$ 0.08	1 $\pm$ 0.04
BUN (mg/dL)	8-33	30.4 $\pm$ 0.64	25.5 $\pm$ 1.63	16.6 $\pm$ 3.29	11.7 $\pm$ 2.11
Creatinine(mg/dL)	0.2-0.9	0.4 $\pm$ 0.31	0.6 $\pm$ 0.14	0.7 $\pm$ 0.16	0.5 $\pm$ 0.04
Glucose (g/dL)	62-175	75.8 $\pm$ 4.71	112.2 $\pm$ 12.41	161.1 $\pm$ 13.12	168.9 $\pm$ 13.12
Cholesterol (mg/dL)	34-219	181.2 $\pm$ 12.16	142.2 $\pm$ 8.12	211.2 $\pm$ 15.12	178.2 $\pm$ 2.77

Mean  $\pm$  SEM

Table 3: Hematological parameters of mice with (i) endometriosis treated with the NPs and (ii) controls.

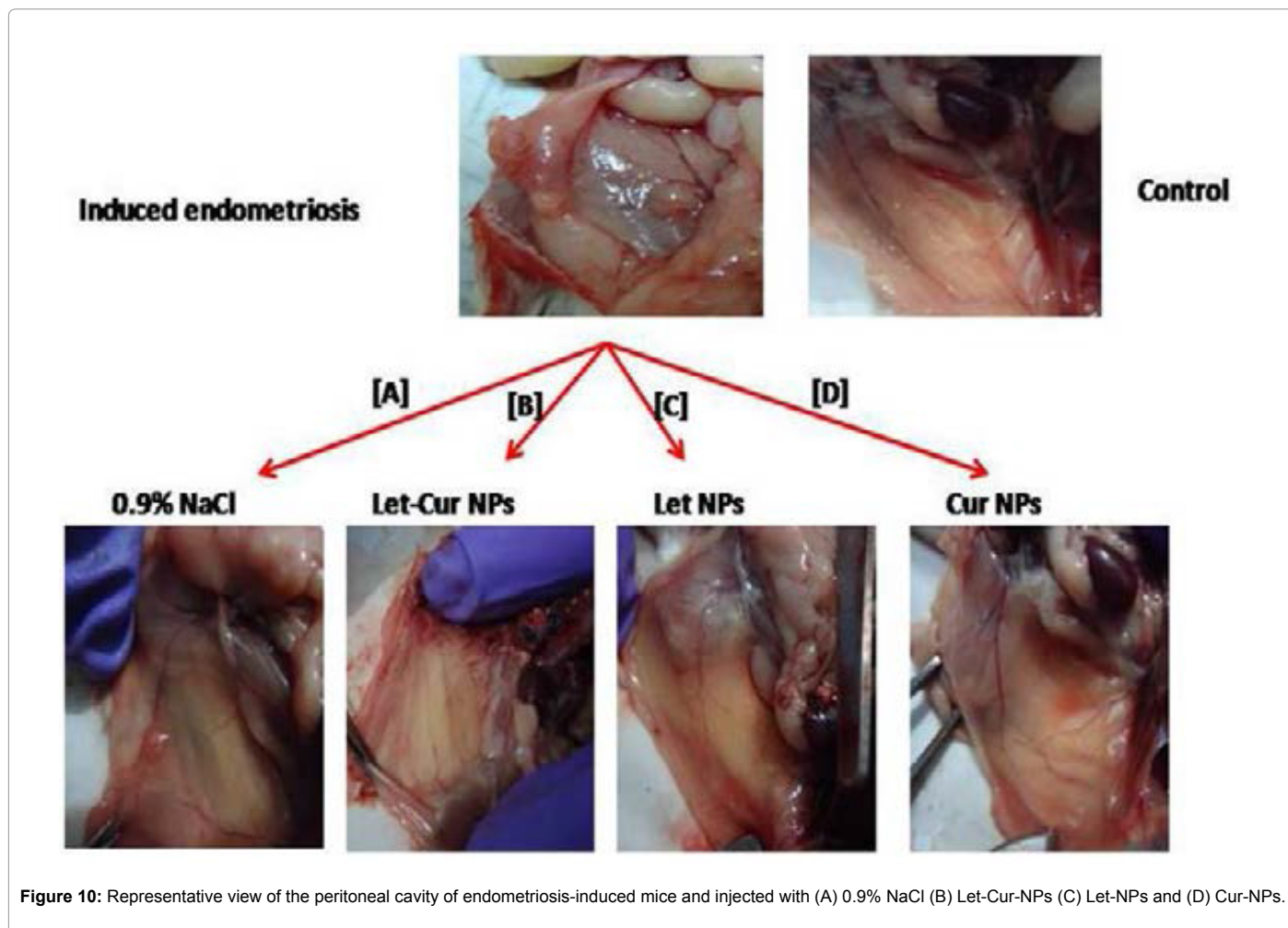


Figure 10: Representative view of the peritoneal cavity of endometriosis-induced mice and injected with (A) 0.9% NaCl (B) Let-Cur-NPs (C) Let-NPs and (D) Cur-NPs.

after administration of Let-Cur-NPs [B] and Let-NPs [C]. Though the lesions decreased to a considerable extent following intraperitoneal

Cur-NPs injection, blood vessels around the endometrial tissue continued to be present [D]. A similar result was observed in tissue immunohistochemistry analysis (Figure 11).

### OS markers, MMPs, VEGF, and E2 estimation

OS markers, MMPs, VEGF, and E2 were estimated in serum of endometriosis induced mice on D20 and significant differences observed on comparing with controls (Table 4). The efficacy of NPs as antioxidant and anti-angiogenic molecule was tested in mice induced with endometriosis. Serum ROS, LPO and TAC levels in various groups of mice are shown in Figure 12. A significant reduction in ROS and LPO and increase in TAC levels were observed after administration of Let-Cur-NPs in mice with endometriosis compared to endometriotic mice injected with 0.9% NaCl (controls). These OS markers showed a similar trend when Cur-NPs were administered to mice with endometriosis; however, it was not surprising to find no significant differences in ROS, LPO and TAC activity following injection of Let-NPs. Figure 13 shows changes in serum MMP2, MMP-9, VEGF and E2 levels following administration of Let- Cur-NPs, Let-NPs and Cur-NPs. While both MMP-2 and E2 levels were found to be comparable before and after Cur-NPs administration, significant changes were seen following injection of Let-NPs and Let-Cur-NPs. Significant changes were also noted in MMP-9 and VEGF before and after administration of all NPs formulation in endometriotic mice.

### Discussion

The conventional treatment regime of endometriosis focuses on lowering the circulating E2 levels, which is effective in alleviating pain and reducing clinical manifestations of the disease. Unfortunately, hypoestrogenism induces many unpleasant side-effects such as hot flashes, uterine spotting and decrease in bone mineral density [21]. As mentioned earlier, aromatase inhibitors such as letrozole are being proposed as the new medical therapy for endometriosis [22]; however, well-designed clinical studies to test the efficacy of these drugs on an adequate sample size are still lacking [23].

OS and ECM degradation are the key processes involved in the pathogenesis of endometriosis [24,25]. In view of this, and also owing to the fact that endometriosis is an E2-dependent disorder, it is logical to presume that development of new therapeutic strategies using a combination of antioxidant molecules and aromatase inhibitors will be useful for effective management of the disease. In an earlier study, we have reported the efficacy of cerium oxide NPs having antioxidant, anti-angiogenic and anti-inflammatory properties on mice with endometriosis. The endometrial lesions reduced significantly accompanied by a decrease in OS. The NPs were also successful in inhibiting VEGF expression and angiogenesis [26]. These findings motivated us to select curcumin as one of NP drug components since cur is well-known for its antioxidant, anti-inflammatory and anti-angiogenic effects. Letrozole, in its nanoparticulate form, was considered as the second combinatorial drug owing to the already existing reports on the drug's ability in decreasing endometriotic lesion size in both humans and animal models. Moreover, there are studies reporting that in vivo bio-distribution of PLGA encapsulated Let-NPs as well as Cur-NPs are non-immunogenic, well tolerated, accumulated in spleen and liver with trace amounts in the lungs and kidneys and virtually none in the heart or brain [27,11]. As discussed earlier, though limited, efficacy of Let-NPs have been tested in endometriosis mice

model, while therapeutic potential of Cur-NPs is yet to be investigated in endometriosis.

Optimization of formulation variables to control the size and drug entrapment efficiency of dual agent-loaded NPs seems to be based on the same scientific principles as single agent-loaded NPs prepared by oil-in- water (O/W) emulsion solvent evaporation method [28]. The emulsification process and stability of emulsion globules are important for the control of particle size; while drug-polymer interaction and the partition of drug in organic phase govern the drug entrapment efficiency. The particle size for the three NP formulations varied between 112 to 132 nm with Let-Cur-NPs having an average size of  $127 \pm 4.51$  nm (Figure 4 and Table 1). The particle size plays an important role in improving the bioavailability of the drug loaded NPs. Smaller particles tend to accumulate in the lesion sites due to facilitated extravasation and hence, greater internalization occurs [29]. The charge of Let-Cur-NPs, Let-NPs and Cur- NPs was estimated to be  $-31.6 \pm 1.91$  mV,  $-31.27 \pm 1.45$  mV and  $-27.47 \pm 1.56$  mV, respectively. The negative zeta potential values are attributed to the fact that free carboxyl groups from PLGA are deprotonated leading to a negatively charged polymer chain. Smaller mean size NPs tend to have a higher zeta potential value as compared to larger NPs. This is so because the small sized

NPs have a higher velocity of migration in a known applied electric field, and hence have a higher zeta potential value, resulting in increased stability of NPs in colloidal dispersions.

FTIR spectra shown in Figure 5 and Table 2 indicate absence of any kind of strong chemical interaction between the drug(s) and the encapsulating polymer PLGA. SEM images evidenced the NPs to be spherical and well-dispersed, as indicated in Figure 6. Biodegradable PLGA polymers are used to facilitate controlled release of a drug from the nano dispersion for sustained drug action. PLGA, being a hydrophilic polymer, can reduce hepatic uptake and improve the circulation half-life of the NPs [28]. Let-Cur-NP formulation indicated a good sustained-release characteristic owing to their high encapsulation efficiency (Figure 9). The rapid "burst" drug release observed in the present study is commonly observed in polymeric NPs *in vitro* [30,31]. It is also concluded that the NPs are biocompatible and do not possess any significant toxicity *in vitro* (Figure 8). Moreover, Cur and Let are proven non-toxic drugs having undergone rigorous human clinical trials [9,22]. For selecting the ideal dose, 40 mg/kg of Let-Cur-NPs was administered in mice every day intra peritoneally and was studied for 7 consecutive days. Subsequently, a dose of 40 mg/kg body wt was selected since no apparent toxic effect or tissue damage was observed at this dose. The number of dead mice increased progressively, 40 mg/kg body wt onwards. The haematological parameters had no obvious changes compared with the saline control group (Table 3) attributing to good biocompatibility and hemocompatibility properties. Significant decrease in endometrial glands, micro-vessels density and CD-34

Molecules	Endometriosis	Controls
ROS (CPS)	269.6±4.12	156.1±5.65
LPO (µMDA)	1.450±0.22	0.7733±0.02
TAC (µM Trolox equivalent)	0.3333±0.02	0.6400±0.04
MMP-2 (ng/ml)	203.3±3.93	146.3±4.7
MMP-9 (ng/ml)	120±2.08	53.67±2.19
VEGF (pg/ml)	7.603±0.21	4.753±0.05
E2 (pg/ml)	44.17±1.86	21.83±0.8172

Mean ± SEM

**Table 4:** ROS, TAC, LPO, MMP-2,-9, VEGF and estrogen (E2) levels in mice with endometriosis and controls before treatment with NPs.



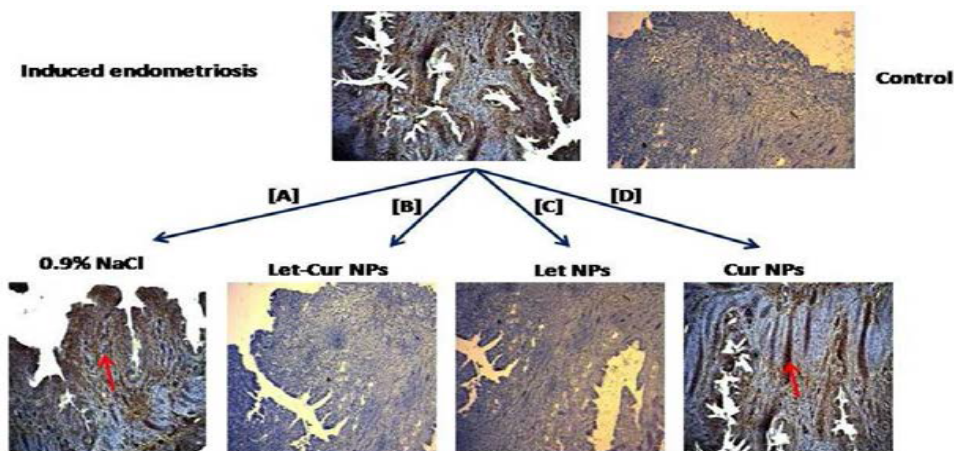


Figure 11: Representative view of tissue immunohistochemistry of mice induced with endometriosis and injected with (A) 0.9% NaCl (B) Let-Cur-NPs (C) Let-NPs and (D) Cur-NPs.

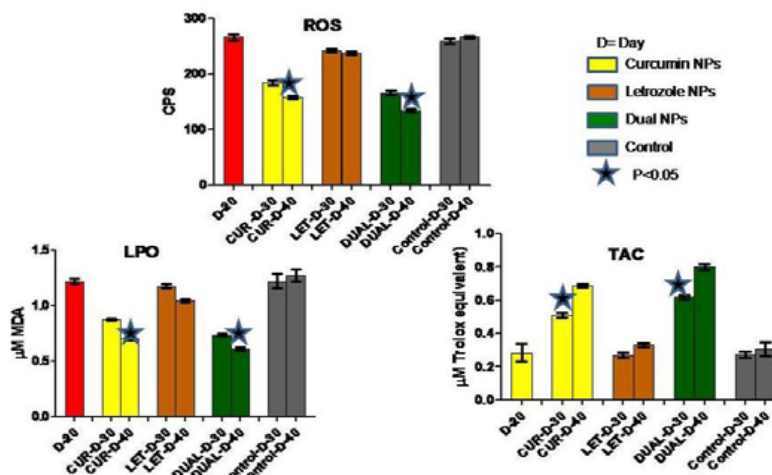


Figure 12: Serum oxidative stress markers including ROS, LPO, and TAC levels in mice with endometriosis before and after treatment with NPs. The red bar depicts mice with endometriosis on D20. The effect of various NPs in different groups on various days is shown.

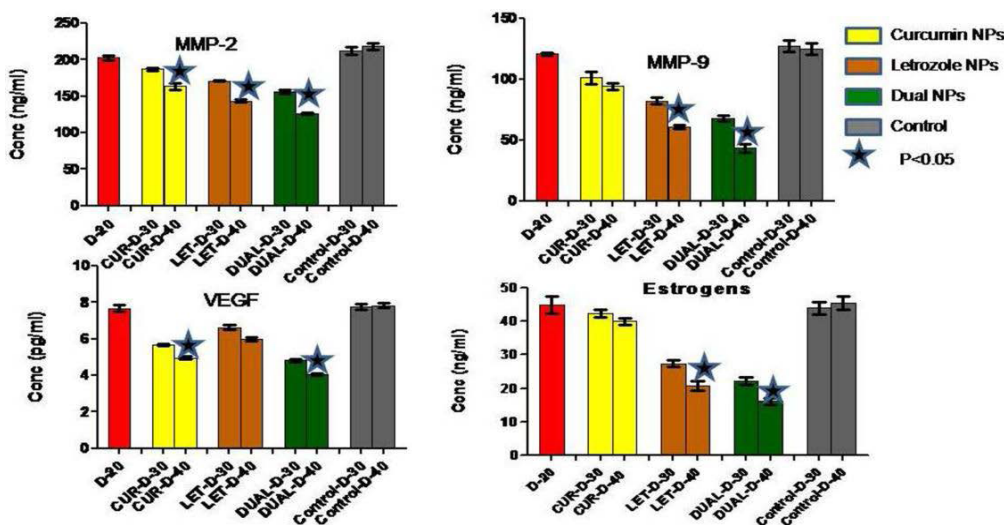


Figure 13: Serum MMP-2, MMP-9, VEGF and E2 levels in mice with endometriosis before and after treatment with NPs.

expression following administration of Let-Cur-NPs as compared to single drug loaded NPs (Let-NPs or Cur-NPs) is observed (Figure 10 and 11). It is interesting to note that the combinatorial effect of Let-Cur-NPs is more effective than single-loaded NPs in terms of reducing OS, estrogenic effect, excessive matrix degradation and angiogenesis in mice with endometriosis (Figure 12 and 13).

This study reports for the first time the combinatorial effect of drug on endometriosis in mice model, where two different drugs, curcumin and letrozole are enclosed in PLGA, known for its low risk of toxicity and sustained release properties. The dual drug NP therapy exerts its anti-estrogenic, anti-inflammatory, anti-angiogenic and antioxidant effect on endometriotic mice in a controlled manner, thereby leading to regression of the disease.

This is a proof of concept study. Pre-clinical non-human primate studies for testing the safety and efficacy of these nanoparticles at larger doses in endometriosis is suggested.

## References

- Jana SK, Banerjee P, Mukherjee R, Chakravarty B, Chaudhury K (2013) HOXA-11 mediated dysregulation of matrix remodeling during implantation window in women with endometriosis. *J Assist Reprod Genet* 30: 1505-1512.
- Guo SW (2009) Recurrence of endometriosis and its control. *Hum Reprod Update* 15: 441-461.
- Antsiferova Y, Sotnikova N, Parfenyuk E (2013) Different Effects of the Immunomodulatory Drug GMDP Immobilized onto Aminopropyl Modified and Unmodified Mesoporous Silica Nanoparticles upon Peritoneal Macrophages of Women with Endometriosis. *Biomed Res Int* 2013:924362.
- Zhao MD, Sun YM, Fu GF, Du YZ, Chen FY, et al. (2012) Gene therapy of endometriosis introduced by polymeric micelles with glycolipid-like structure. *Biomaterials* 33: 634-643.
- Jana SK, Dutta M, Joshi M, Srivastava S, Chakravarty B, et al. (2013) <sup>1</sup>H NMR based targeted metabolite profiling for understanding the complex relationship connecting oxidative stress with endometriosis. *Biomed Res Int* 2013: 329058.
- Ngô C, Chéreau C, Nicco C, Weill B, Chapron C, et al. (2009) Reactive oxygen species controls endometriosis progression. *Am J Pathol* 175: 225-234.
- Patil TN, Srinivasan M (1971) Hypocholesteremic effect of curcumin in induced hypercholesteremic rats. *Indian J Exp Biol* 9: 167-169.
- Bisht S, Feldmann G, Soni S, Ravi R, Karikar C, et al. (2007) Polymeric nanoparticle-encapsulated curcumin (nanocurcumin): a novel strategy for human cancer therapy. *J Nanobiotechnology* 5: 3.
- Anand P, Kunnumakkara AB, Newman RA, Aggarwal BB (2007) Bioavailability of curcumin: problems and promises. *Mol Pharm* 4: 807-818.
- Mathew A, Fukuda T, Nagaoka Y, Hasumura T, Morimoto H, et al. (2012) Curcumin loaded-PLGA nanoparticles conjugated with Tet-1 peptide for potential use in Alzheimer's disease. *PLoS One* 7: e32616.
- Zou P, Helson L, Maitra A, Stern ST, McNeil SE (2013) Polymeric curcumin nanoparticle pharmacokinetics and metabolism in bile duct cannulated rats. *Mol Pharm* 10: 1977-1987.
- Ailawadi RK, Jobanputra S, Kataria M, Gurates B, Bulun SE (2004) Treatment of endometriosis and chronic pelvic pain with letrozole and norethindrone acetate: a pilot study. *Fertil Steril* 81: 290-296.
- Ferrero S, Venturini PL, Ragni N, Camerini G, Remorgida V (2009) Pharmacological treatment of endometriosis: experience with aromatase inhibitors. *Drugs* 69: 943-952.
- Verma A, Konje JC (2009) Successful treatment of refractory endometriosis-related chronic pelvic pain with aromatase inhibitors in premenopausal patients. *Eur J Obstet Gynecol Reprod Biol* 143: 112-115.
- Oner G, Ozcelik B, Ozgun MT, Serin IS, Ozturk F, et al. (2010) The effects of metformin and letrozole on endometriosis and comparison of the two treatment agents in a rat model. *Hum Reprod* 25: 932-937.
- Lehár J, Krueger AS, Avery W, Heilbut AM, Johansen LM, et al. (2009) Synergistic drug combinations tend to improve therapeutically relevant selectivity. *Nat Biotechnol* 27: 659-666.
- Mora-Huertas CE, Fessi H, Elaissari A (2010) Polymer-based nanocapsules for drug delivery. *Int J Pharm* 385: 113-142.
- Nowak NM, Fischer OM, Gust TC, Fuhrmann U, Habenicht UF, et al. (2008) Intraperitoneal inflammation decreases endometriosis in a mouse model. *Hum Reprod* 23: 2466-2474.
- Buege JA, Aust SD (1978) Microsomal lipid peroxidation. *Methods Enzymol* 52: 302-310.
- Chapple IL (1997) Reactive oxygen species and antioxidants in inflammatory diseases. *J Clin Periodontol* 24: 287-296.
- Helms RA, D.J Q (2006) Textbook of therapeutics: drug and disease management Philadelphia Lippincott Williams & Wilkins.
- Ferrero S, Gillott D, Venturini P, Remorgida V (2011) Use of aromatase inhibitors to treat endometriosis-related pain symptoms: a systematic review. *Reproductive Biology and Endocrinology* 9:89.
- Alborzi S, Hamed B, Omidvar A, Dehbashi S, Alborzi M (2011) A comparison of the effect of short-term aromatase inhibitor (letrozole) and GnRH agonist (triptorelin) versus case control on pregnancy rate and symptom and sign recurrence after laparoscopic treatment of endometriosis. *Arch Gynecol Obstet* 284:105-110.
- Augoulea A, Mastorakos G, Lambrinoudaki I, Christodoulakos G, Creatsas G (2009) The role of the oxidative-stress in the endometriosis-related infertility. *Gynecol Endocrinol* 25: 75-81.
- Healy DL, Rogers PA, Hii L, Wingfield M (1998) Angiogenesis: a new theory for endometriosis. *Hum Reprod Update* 4: 736-740.
- Chaudhury K, Babu KN, Singh AK, Das S, Kumar A, et al. (2012) Mitigation of endometriosis using regenerative cerium oxide nanoparticles. *Nanomedicine: Nanotechnology, Biology and Medicine* 9: 439-448.
- Mondal N, Halder KK, Kamila MM, Debnath MC, Pal TK, et al. (2010) Preparation, characterization, and biodistribution of letrozole loaded PLGA nanoparticles in Ehrlich Ascites tumor bearing mice. *Int J Pharm* 397: 194-200.
- Danhier F, Ansorena E, Silva JM, Coco R, Le Breton A, et al. (2012) PLGA-based nanoparticles: an overview of biomedical applications. *J Control Release* 161: 505-522.
- Yuan F, Leunig M, Huang SK, Berk DA, Papahadjopoulos D, et al. (1994) Microvascular permeability and interstitial penetration of sterically stabilized (stealth) liposomes in a human tumor xenograft. *Cancer Res* 54: 3352-3356.
- Danhier F, Lecouturier N, Vroman B, Jerome C, Marchand-Brynaert J, et al. (2009) Paclitaxel-loaded PEGylated PLGA-based nanoparticles: in vitro and in vivo evaluation. *J Control Release* 133: 11-17.
- Zhang L, Hu Y, Jiang X, Yang C, Lu W, et al. (2004) Camptothecin derivative-loaded poly(caprolactone-co-lactide)-b-PEG-b-poly(caprolactone-co-lactide) nanoparticles and their biodistribution in mice. *J Control Release* 96: 135-148.